Journal of Power Sources 227 (2013) 101–105

Contents lists available at SciVerse ScienceDirect

Journal of Power Sources

journal homepage: www.elsevier.com/locate/jpowsour

Short communication

Facile synthesis of hollow Co_3O_4 boxes for high capacity supercapacitor

Wei Du [a,b], Rongmei Liu [a,b,c], Yuanwen Jiang [a], Qingyi Lu [a,*], Yongzhang Fan [a,b], Feng Gao [b,**]

[a] State Key Laboratory of Coordination Chemistry, Coordination Chemistry Institute, Nanjing National Laboratory of Microstructures, School of Chemistry and Chemical Engineering, Nanjing University, Nanjing 210093, PR China
[b] Department of Materials Science and Engineering, Nanjing University, Nanjing 210093, PR China
[c] College of Biological and Chemical Engineering, Anhui Polytechnic University, Wuhu Anhui 241000, PR China

HIGHLIGHTS

- Cobalt acetate hydroxide prisms were obtained by a low temperature re-crystallization process.
- Hollow Co_3O_4 boxes were obtained by calcining cobalt acetate hydroxide prisms in air.
- Hollow Co_3O_4 structures exhibit wonderful capacitive properties.

ARTICLE INFO

Article history:
Received 18 June 2012
Received in revised form
22 October 2012
Accepted 7 November 2012
Available online 13 November 2012

Keywords:
Cobalt oxide
Hollow structures
Kirkendall effect
Supercapacitor

ABSTRACT

One-dimensional (1D) cobalt acetate hydroxide ($Co_5(OH)_2(CH_3COO)_8 \cdot 2H_2O$) prisms has been obtained through a low temperature re-crystallization process in the dissolvant of ethanol and then transferred to cobalt oxide by calcining in the air. Cobalt oxide keeps the outside configuration of the 1D cobalt acetate hydroxide but turns to be boxes with hollow structure inside through the Kirkendall effect. The precursor prisms and polycrystalline boxes both have length of about 3 μm, width of 300 nm and height of 300 nm characterized by X-ray powder diffraction (XRD), scanning electron microscopy (SEM) and transmission electron microscopy (TEM). The electrochemical measurement results show that the hollow Co_3O_4 structures exhibit wonderful capacitive properties with high capacitance and good cyclicity.

© 2012 Elsevier B.V. All rights reserved.

1. Introduction

Energy problems have undoubtedly become the greatest problems and attracted worldwide attention in the modern society [1,2]. Searching for new materials possessing great performances in dealing with the energy conversion, storage and usage has been proved to be an important task for every scientific worker [3,4]. Supercapacitor, a new energy storage device, has many advantages such as long service life, great power density, high energy density, green environmental protection and has attracted enormous research interest in the recent years. Active materials in electrodes of supercapacitors have great effects on electrochemical performance and capacity of energy storage devices and looking for new electrode materials has become a key issue for the supercapacitor development. Cobalt oxide, as an important transition metal oxide, has great application potentials in many fields such as lithium-ion batteries and heterogeneous catalysis due to its low-cost and environmental friendly nature [5]. Recently, cobalt oxide has been applied in supercapacitors as electrode material and proved to be a potential alternate to expensive RuO_2, which are used broadly as an electrode material but costs too high to be accepted [5–10].

Nanomaterials with hollow structures can be potentially applied in many fields because of the unique structure could provide fast ion and electron transfer, large reaction surface area and good strain accommodation [11]. The specific surface area of the active nanomaterials in electrode would have great influences on the capacitance, which makes hollow structures might have great application potentials in supercapacitor. Until now, the common used synthesis methods for hollow structures are template-method and water/oil/water (W/O/W) emulsion-system. However, the removal of template, the preparation conditions of water/oil/water and the usage of precipitants are usually troublesome and time-wasted [12]. So, it is very necessary for materials scientists to look for a simple and effective method to synthesize hollow-structures. In the study presented here, we developed a simple

* Corresponding author. Tel.: +86 25 83685773; fax: +86 25 83314502.
** Corresponding author.
E-mail addresses: qylu@nju.edu.cn (Q. Lu), fgao@nju.edu.cn (F. Gao).

0378-7753/$ – see front matter © 2012 Elsevier B.V. All rights reserved.
http://dx.doi.org/10.1016/j.jpowsour.2012.11.009

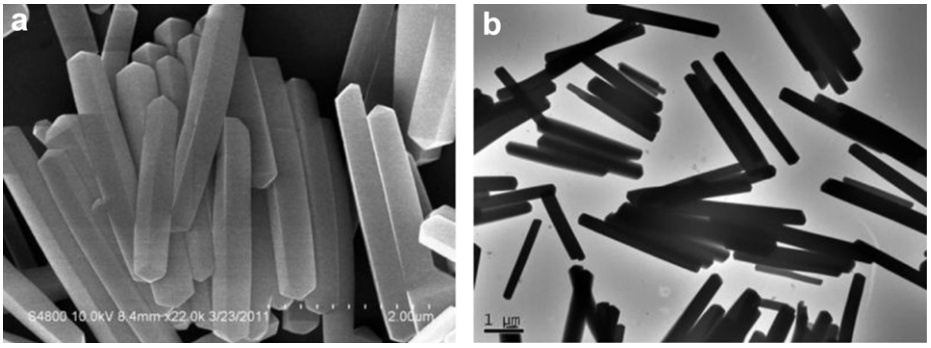

Fig. 1. (a) FESEM and (b) TEM images of the precursor prisms.

and convenient approach and successfully obtained hollow Co_3O_4 nanostructures through a precursor route without the use of any surfactants or templates. What is mentionable is that the precursor ($Co_5(OH)_2(CH_3COO)_8 \cdot 2H_2O$) was easily obtained from the solution of $Co(CH_3COO)_2 \cdot 4H_2O$ in ethanol at a low temperature through a re-crystallization process. The precursor is uniform one-dimensional prisms with a length of about 3 μm, a width of 300 nm and a height of 300 nm. The precursor was transferred to Co_3O_4 structures by thermal decomposition and unlike the precursor, the obtained Co_3O_4 structures are hollow boxes, which can be attributed to the Kirkendall effect. The resulting hollow cobalt oxide boxes were found to exhibit outstanding supercapacitive properties, possessing high specific capacitances and excellent cycle stability.

2. Experimental

All chemicals were of analytical grade and used as received without further purification. In a typical synthesis, 0.8 g of cobalt acetate tetrahydrate ($Co(CH_3COO)_2 \cdot 4H_2O$) was dissolved in 500 mL of cold ethanol and kept at −5 °C for days. The precipitation was collected and washed with ethanol for several times by a centrifugation–redispersion process. Then the final product was dried in an oven at 40 °C for 4 h. For the synthesis of Co_3O_4 structures, the as-prepared precursor was heated to 300 °C with a ramping rate of 1 °C min^{-1} and kept for 10 min in the air.

2.1. Characterizations

Crystallographic phases of all the products were investigated by powder X-ray diffraction (XRD) on Switzerland ARL X'TAR with Cu K_α irradiation (λ = 1.5406 Å). Morphologies of samples were observed by field emission scanning electron microscopy (SEM; Hitachi S-4800), and transmission electron microscopy (TEM; JEM-2100) with selected area electron diffraction (SAED). Thermal behaviors of samples were characterized by thermogravimetric analysis (TGA; a NETZSCH STA 449 F3 Jupiter simultaneous thermal analyzer) at a heating rate of 5 °C min^{-1} from room temperature to 600 °C in air.

2.2. Electrochemical measurements

In the electrochemical experiments, we used the traditional three electrode system. The working electrode was prepared by mixing 80 wt% of electroactive material (Co_3O_4), 10 wt% of acetylene black, and 10 wt% of polytetrafluoroethylene. This mixture was then pressed onto the foamed nickel electrode and dried at 60 °C for 12 h. The used electrolyte was 3% KOH aqueous solution. The capacitive performance of the samples was evaluated on a CHI 660d electrochemical workstation. Cyclic voltammetry and chronopotentiometry were tested with a three-electrode cell where Pt foil serves as the counter electrode and a standard calomel electrode (SCE) as the reference electrode.

3. Results and discussion

The synthesis involves two steps, the formation of the precursor and subsequent thermal conversion to Co_3O_4 under controlled conditions. The precursor was prepared by dissolving cobalt acetate tetrahydrate in cold ethanol and then precipitated from the solution. Fig. 1a shows an SEM image of the as-prepared precursor. It can be observed that it consists of uniform prisms with about 3 μm in length, 300 nm in width and 300 nm in height. To the best of our knowledge, this type of Co-based structure has not been reported before, as the 3D architectures demonstrated previously are generally cubic [13]. Fig. 1b displays a TEM image of the precursor and confirms that the obtained product is one-dimension prisms with uniform sizes. It can be also clearly seen that they are solid and do not have hollow structure. The phase composition of the precursor was investigated by XRD. Fig. 2a shows the XRD pattern of the obtained precursor while Fig. 2b displays the XRD pattern of cobalt acetate hydroxide which was converted from ".cif" file from the literature [14] using MERCURY software. By comparing the two XRD patterns, it can be easily deduced that the obtained precursor is cobalt acetate hydroxide $Co_5(OH)_2(CH_3COO)_8 \cdot 2H_2O$. The cobalt

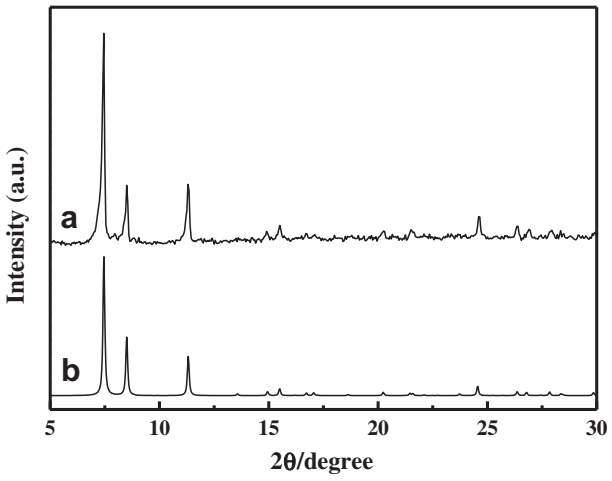

Fig. 2. XRD patterns of (a) the as-prepared precursor and (b) $Co_5(OH)_2(OOCCH_3)_8 \cdot 2H_2O$ simulated by using the published crystal cif file through Mercury software.

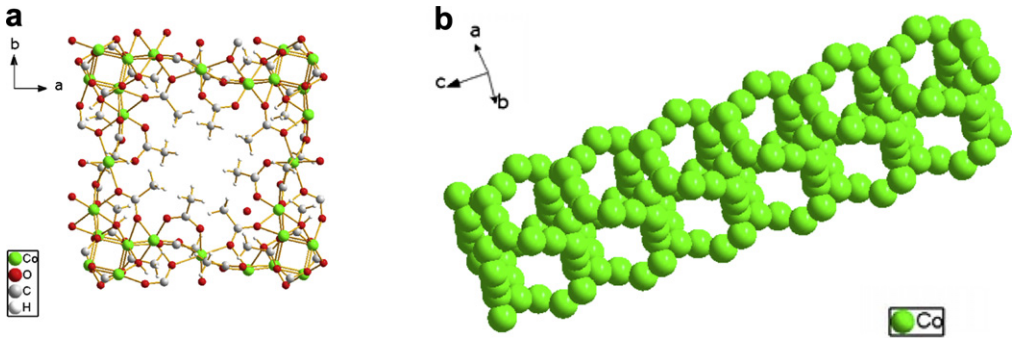

Fig. 3. 3D Crystal cell accumulation figure (a) viewed along the *c*-axis and (b) viewed after a small spin.

acetate hydroxide belongs to tetragonal with the cell length ($a = b = 23.693$ Å, $c = 11.565$ Å) and cell angle ($\alpha = \beta = \gamma = 90°$). Fig. 3a presents the schematic crystal structure of $Co_5(OH)_2(CH_3COO)_8 \cdot 2H_2O$ unit cell projected along the *c* axis and Fig. 3b displays a schematic crystal structure of $Co_5(OH)_2(CH_3COO)_8 \cdot 2H_2O$ super cell ($0.5 \times 0.5 \times 6$ slabs). Based on the crystal structure, we could easily deduce that the compound might grow along *c* axis to become a prism with similar width and height. During this process, $Co(CH_3COO)_2 \cdot 4H_2O$ was first dissolved in ethanol and formed a pink transparent solution. The small amount of crystallization water from $Co(CH_3COO)_2 \cdot 4H_2O$ would make $Co(CH_3COO)_2$ hydrolyze slowly in ethanol and $Co_5(OH)_2(CH_3COO)_8 \cdot 2H_2O$ would recrystallized from the solution. This chemical process could be described as the follow equation and the formation of CH_3COOH can be verified by the acidity increase of the resulting solution.

$$5Co(CH_3COO)_2 + 4H_2O \rightarrow Co_5(OH)_2(CH_3COO)_8 \cdot 2H_2O + 2CH_3COOH$$

Usually, the cobalt compound is thermally unstable and decomposes at a temperature below 300 °C to convert to stable Co_3O_4 in the air [15,16]. Fig. 4 gives the TGA curve in air of the precursor. After the loss of H_2O at about 100 °C, a weight loss begins at about 250 °C, indicating the onset of oxidation. Based on the TGA data, the precursor prisms were annealed in air at 300 °C to transfer to cobalt oxide. Fig. 5 presents the XRD pattern of the product obtained by annealing the precursor at 300 °C. It can be perfectly indexed to cubic spinel Co_3O_4 (JCPDS card no. 43-1003, space group: Fd3m (227), $a = 8.084$ Å), indicating that the as-synthesized Co-based precursor prisms have been completely converted to phase-pure spinel Co_3O_4. Fig. 6a shows the SEM image of the product after heat treatment. It can be seen that the 1D prism morphology of the precursor is maintained very well. But unlike the precursor, these 1D crystals are hollow boxes, which can be clearly seen as there are holes of the broken ends. The surface of the boxes is very rough, suggesting that the boxes might be composed of Co_3O_4 nanoparticles. The TEM image shown in Fig. 6b demonstrates that the product has hollow box-like structure with uniform length, width and height and the Co_3O_4 boxes are composed of nanoparticles, which leads to the polycrystalline SAED pattern (Fig. 6b right-up-inset). The crystalline nature of Co_3O_4 boxes was confirmed by a high-resolution HRTEM image (Fig. 6b right-down-inset), which displays clear lattices of Co_3O_4 crystal. Hollow porous structures of Co_3O_4 were obtained during the slow heating process, which might be an application of the Kirkendall effect [11,17,18]. During the annealing process in air, the oxidation of C, H, and Co would happen firstly at the surface of the precursor. A layer of Co_3O_4 would form at the surface and the freshly exposed C, H, and Co would move to the surface to react with oxygen in air. Then with continuous evacuation of the core $Co_5(OH)_2(CH_3COO)_8 \cdot 2H_2O$ to surface, inner cavities would eventually form and leads to the formation of the hollow Co_3O_4 boxes.

Co_3O_4 has been extensively researched as the electrode material for lithium-ion batteries and supercapacitors [15,19,20]. In this paper we studied the electrochemical properties of obtained Co_3O_4 boxes by applying it as the active material for supercapacitor electrode. For comparison, the electrochemical properties of

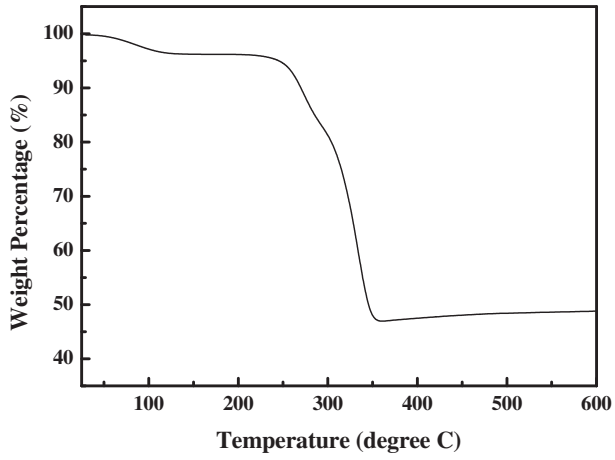

Fig. 4. Thermogravimetric analysis (TGA) curve of the precursor in air.

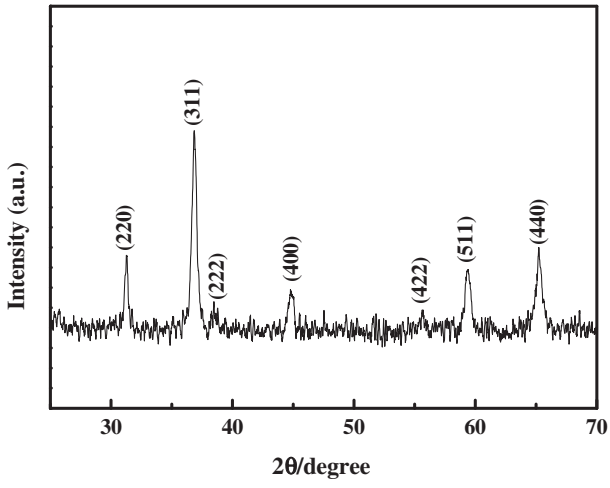

Fig. 5. XRD pattern of the Co_3O_4 structures by calcining the precursor at 300 °C.

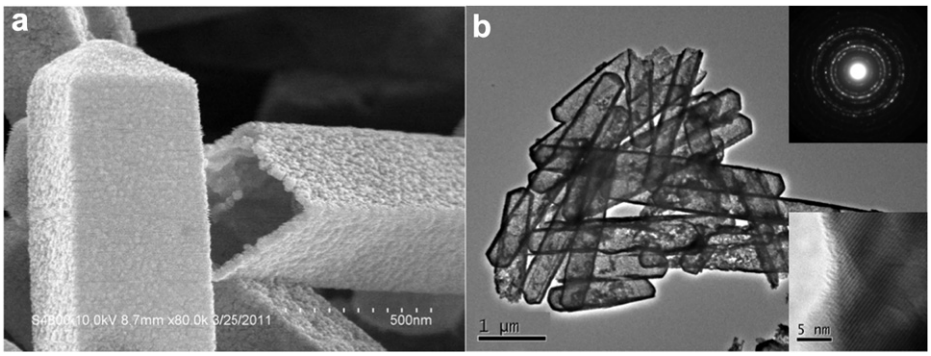

Fig. 6. (a) SEM and (b) TEM images of Co_3O_4 boxes obtained by calcining the precursor prisms (inset: HRTEM image and SAED pattern).

commercial cobalt oxide were also studied. The measurements are conducted using cyclic voltammetry (CV) in 3% KOH electrolyte with the voltage window in 0–0.5 V and a scanning rate of 5 mv s^{-1}. The obtained CV curves are shown in Fig. 7a. The CV curves are nearly symmetrical and display two pairs of redox peaks. The broad redox reaction peaks which come from the redox processes of Co_3O_4/CoOOH/CoO_2, are characters of the electrochemical pseudocapacitors from reversible faradaic redox reactions occurring within the electro-active materials [21,22]. The area under the CV curve for Co_3O_4 boxes is apparently much larger than that of commercial Co_3O_4, which indicates that Co_3O_4 boxes have a higher specific capacitance than commercial Co_3O_4. This is reasonable since the unique structure of Co_3O_4 could provide fast ion and electron transfer and large reaction surface area, benefiting for the electrochemical performance. Chronopotentiometry measurements confirm the suggestions. Fig. 7b shows charge–discharging curves of Co_3O_4 boxes and commercial Co_3O_4 powders obtained in potential range of 0–0.5 V in 3% KOH at a charging–discharging current of 0.5 A g^{-1}. The shapes of the charge–discharge curves do not show the characteristics of pure double-layer capacitor, but mainly pseudo-capacitance [10], which are in agreement with the result of the CV curves. Both samples present two variation ranges during the charge and discharge steps. The sloped curve in 0.32–0.5 V is characteristic of typical pseudocapacitance, originating from electrochemical adsorption–desorption or a redox reaction on the electrode/electrolyte interface. From the sloped curve at the discharge current of 0.5 A g^{-1}, the specific capacitances of Co_3O_4 boxes and commercial Co_3O_4 powders are calculated to be 278 F g^{-1}

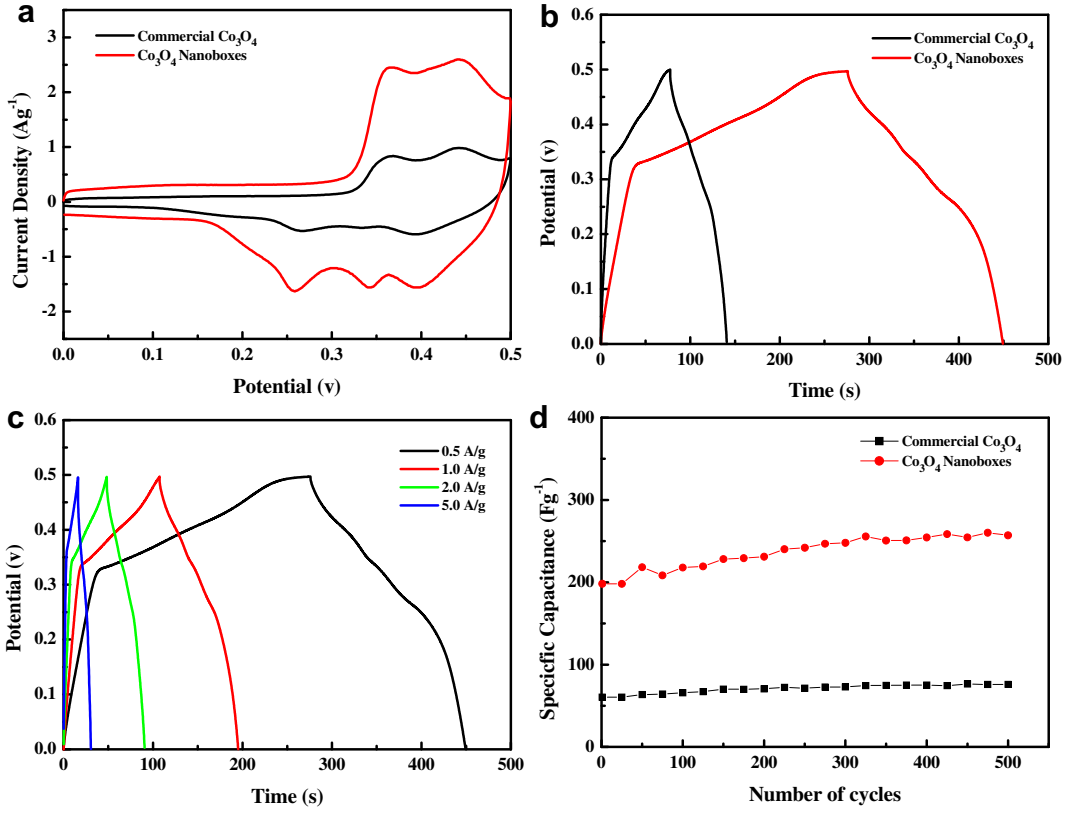

Fig. 7. (a) CV curves of the Co_3O_4 boxes and commercial Co_3O_4 in the potential region of 0.1–0.5 V at a scanning rate of 5 mv s^{-1}; (b) Charge–discharge curves of Co_3O_4 boxes and commercial Co_3O_4 at current density of 0.5 A g^{-1} (c) Charge–discharge curves of the Co_3O_4 boxes at different current densities of 0.5, 1, 2, and 5 A g^{-1}; (d) Cycling performances of Co_3O_4 boxes and commercial Co_3O_4 at current density of 2 A g^{-1}.

and 77 F g^{-1}, respectively. The specific capacitance of Co_3O_4 boxes is much larger than that of commercial Co_3O_4 powders, confirming the suggestion rising from the CV curves. When the discharge current density is 0.5, 1, 2 and 5 A g^{-1}, the specific capacitance values of the Co_3O_4 boxes can be calculated from the discharge curves to be 278 F g^{-1}, 216 F g^{-1}, 198 F g^{-1} and 176 F g^{-1}, which can be calculated from Fig. 7c, respectively. Although there are some reports showing much higher specific capacitances for Co_3O_4, as mentioned in the introduction, specific surface area of the active nanomaterials in electrode would have great influence on the capacitance. Brunauer–Emmett–Teller (BET) gas-sorption measurements of the Co_3O_4 boxes were performed. Based on the BET gas-sorption measurement, the BET specific surface area of the obtained Co_3O_4 nanoboxes is 31.07 m^3 g^{-1}, much smaller than that of mesoporous aerogels Co_3O_4 solid square (235 m^2 g^{-1}), which shows a high specific capacitance of 623 F g^{-1} [5]. However, with the similar specific surface area, the obtained Co_3O_4 nanoboxes show a higher capacitance than hexagonal Co_3O_4 nanosheets [10], which may be due to the hollow structure.

As a long cycle life is very important for supercapacitors, the cycle charge/discharge test has also been employed to examine the service life of the Co_3O_4 boxes. Fig. 7d shows the variation of specific capacitance with cycle number at 2 A g^{-1} and reveals that the Co_3O_4 boxes electrode has good cycle properties as an excellent electrode material for electrochemical capacitors and the specific capacitance even grow a little larger in the first 500 cycles, which might be due to an electrochemical activation phenomenon [23]. Clearly, Co_3O_4 box electrode holds better electrochemical capacitance performances than the commercial Co_3O_4 electrode. The high porosity structure of Co_3O_4 boxes minimizes both the ionic and electronic transportation distances in the Co oxide and thus improves the electrode kinetic performance, which is a crucial concern for high-power supercapacitor applications.

4. Conclusions

In summary, we have successfully demonstrated a simple fabrication route for 1D Co_3O_4 hollow structure via a controlled thermolysis of the precursor. The 1D precursor was easily obtained through a re-crystallization process from $Co(CH_3COO)_2$ ethanol solution at low temperature and transferred to Co_3O_4 boxes by Kirkendall effect. Our findings would provide a deeper understanding of the concept and application of the Kirkendall effect as a straightforward processing protocol for hollow structure. This approach enables the promising prospect that a variety of organometallic coordination compound precursors will be accessible for widespread applications of Kirkendall effect to get hollow structure. The electrochemical measurements reveal that the Co_3O_4 boxes manifest promising pseudo-capacitive properties with high capacitance and good cyclicity. We believe that these active Co_3O_4 materials with distinct structures could serve as promising candidates in other applications, such as catalysis and lithium-ion batteries.

Acknowledgment

This work is supported by the National Basic Research Program of China (Grant No. 2011CB935800 and 2013CB922102), the National Natural Science Foundation of China (Grant No. 21071076, 21021062, and 51172106) and the Natural Science Foundation of Jiangsu Province (Grant No. BK2010370).

References

[1] M. Winter, R.J. Brodd, Chem. Rev. 104 (2004) 4245.
[2] T.Y. Wei, C.H. Chen, H.C. Chien, S.Y. Lu, C.C. Hu, Adv. Mater. 22 (2010) 347.
[3] M. Armand, J.M. Tarascon, Nature 451 (2008) 652.
[4] M.Z. Jacobson, Energy Environ. Sci. 2 (2009) 148.
[5] T.Y. Wei, C.H. Chen, K.H. Chang, S.Y. Lu, C.C. Hu, Chem. Mater. 21 (2009) 3228.
[6] C.C. Hu, K.H. Chang, M.C. Lin, Y.T. Wu, Nano Lett. 6 (2006) 2690.
[7] S.G. Kandalkar, C.D. Lokhande, R.S. Mane, S.H. Han, Appl. Surf. Sci. 253 (2007) 3952.
[8] A.B. Yuan, Q.L. Zhang, Electrochem. Commun. 8 (2006) 1173.
[9] H. Pang, F. Gao, Q. Chen, R.M. Liu, Q.Y. Lu, Dalton Trans. 41 (2012) 5862.
[10] S.L. Xiong, C.Z. Yan, X.G. Zhang, B.J. Xi, Y.T. Qian, Chem. Eur. J. 15 (2009) 5320.
[11] C.C. Park, Y. Cho, K. Kim, J. Kim, M.L. Liu, J. Cho, Angew. Chem. Int. Ed. 50 (2011) 9647.
[12] M. Fujiwara, K. Shiokawa, Y. Tanaka, Y. Nakahara, Chem. Mater. 16 (2004) 5420.
[13] F. Cao, D.Q. Wang, R.P. Deng, J.K. Tang, S.Y. Song, Y.Q. Lei, S. Wang, S.Q. Su, X.G. Yang, H.G. Zhang, CrystEngComm 13 (2011) 2123.
[14] R. Kuhlman, G.L. Schimek, J.W. Kolis, Inorg. Chem. 38 (1999) 194.
[15] T. Zhu, J.S. Chen, X.W. Lou, J. Mater. Chem. 20 (2010) 7015.
[16] Z.P. Xu, H.C. Zeng, J. Mater. Chem. 8 (1998) 2499.
[17] B. Liu, H.C. Zeng, J. Am. Chem. Soc. 126 (2004) 16744.
[18] J.X. Wang, C. Ma, Y.M. Choi, D. Su, Y.M. Zhu, P. Liu, R. Si, M.B. Vukmirovic, R.R. Adzic, J. Am. Chem. Soc. 133 (2011) 13551.
[19] Y.G. Li, B. Tan, Y.Y. Wu, Nano Lett. 8 (2008) 265.
[20] X.H. Xia, J.P. Tu, Y.J. Mai, X.L. Wang, C.D. Gu, X.B. Zhao, J. Mater. Chem. 21 (2011) 9319.
[21] S. Palmas, F. Ferrara, A. Vacca, M. Mascia, A.M. Polcaro, Electrochim. Acta 53 (2007) 400.
[22] G.L. Wang, D.X. Cao, C.L. Yin, Y.Y. Gao, J.L. Yin, L. Cheng, Chem. Mater. 21 (2009) 5112.
[23] C.C. Hu, K.H. Chang, T.Y. Hsu, J. Electrochem. Soc. 155 (2008) F196.